

A MEMS-Based, High-Sensitivity Pressure Sensor for Ultraclean Semiconductor Applications

Albert K. Henning, Nicholas Mourlas, and Steven Metz
Redwood Microsystems, Inc.
959 Hamilton Avenue
Menlo Park, CA 94025
USA
henning@redwoodmicro.com

Art Zias
ZiaSense
941 Oxford Drive
Los Altos, CA 94024
USA
ziasense@earthlink.net

Abstract

Process applications in the semiconductor industry require increasing levels of performance in pressure measurement and control. In addition, measurement and control of process mass flows are moving toward pressure-based mass flow controllers (MFCs). This work reports the development of a MEMS-based pressure sensor, with the requisite performance for rigorous pressure and flow sensing. The pressure sensing element consists of two capacitor plates, whose separation varies as a function of the radial distance from the center of the structure. The bottom capacitor plate is mechanically fixed, while the upper plate is a flexible silicon membrane. A variable separation between the plates is introduced by locating a hub in the center of the structure, and stretching the membrane over this structure. The theoretical principles, fabrication and performance of the structure are discussed.

Keywords

Pressure sensor; mass flow controller (MFC) microelectromechanical system (MEMS); process gas control and distribution

1. Introduction

A wide variety of process applications in the semiconductor industry require pressure measurement and control. Increasingly, the level of performance demanded from ultraclean pressure sensors and transducers has grown. Applications from electrostatic chuck temperature and pressure control, to ion implantation chamber pressure regulation, to low pressure chemical vapor deposition, require improvements in pressure measurement resolution and drift. In addition, measurement and control of process mass flows are moving toward pressure-based mass flow controllers

(MFCs), and away from thermal MFCs, in order to create process flow environments which are insensitive to fluctuations in system pressures either upstream or downstream of the process chamber.

Silicon micromachined pressure sensors can be divided into two general classes: piezoresistive [1], where a diffused resistor bridge in a flexible membrane generates a pressure-dependent voltage; and capacitive [2], where the capacitance between the flexible membrane and a fixed plate changes as a function of pressure. Most piezoresistive and capacitive sensors are designed and signal conditioned to behave roughly linearly in pressure. This aspect was important in an era of analog signal processing, where linearity was an essential attribute of a stable and repeatable system. These sensor designs led to a roughly constant accuracy as a percent of sensor *full-scale*, but limited the dynamic range over which this accuracy could be assured. Present-day electronics technology increasingly relies on embedded systems utilizing digital signal processing. Applications utilizing such technology could benefit greatly from sensors with a wider dynamic range, which traditional piezoresistive and capacitive sensors do not afford.

In this work, we report the development of a MEMS-based pressure sensor, with the requisite performance for these rigorous pressure sensing and flow sensing applications. It has a wide, but not necessarily linear, dynamic range. As a consequence, the sensor enables development of a finished pressure transducer, with a wide dynamic range, and accuracy which is roughly constant as a percent of *reading*, over the full operating range of the device. The sensor is facilitated by a novel structure. The novelty stems from two aspects: the *shape* of the flexible membrane changes in a well-described, non-linear manner as a function of pressure; and, the *initial tension* of the flexible membrane (which plays an

important role in controlling the shape) is defined by a choice of well-defined processing parameters.

Specifically, the pressure sensing element consists of two capacitor plates, whose separation varies as a function of the radial distance from the center of the structure (see Figure 1a) [3]. The bottom (substrate) capacitor plate is mechanically fixed, while the upper (membrane) plate is a flexible silicon membrane. The variable separation between the plates is facilitated by locating a hub in the center of the structure, and stretching the membrane over this structure. The process of stretching the membrane over the hub results in a vacuum in the sealed cavity between the two capacitor plates.

The sealed cavity can have its pressure set arbitrarily. As a consequence, the pressure of greatest sensitivity can be 'tuned' during the sensor manufacturing process. External pressures on the flexible electrode greater than this reference pressure cause the membrane to deflect toward the fixed electrode (see Figure 1b).

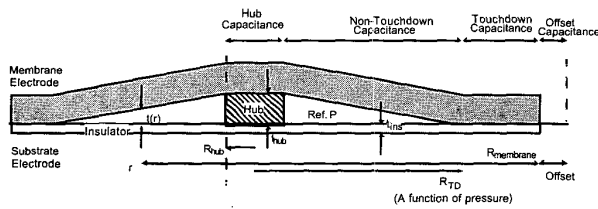


Figure 1a: Schematic of the pressure sensor's capacitor structure, and variables related to the modeled capacitance vs. pressure behavior.

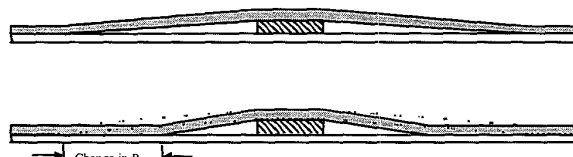


Figure 1b: Schematic of the pressure sensor at equilibrium (top), where the external pressure equals the reference pressure; and under active load (bottom), where the external pressure exceeds the reference pressure.

2. Theoretical Principles

The membrane, upon exposure to absolute pressures above vacuum, deforms elastically and reproducibly. The exact nature of the deformation, as a function of the applied pressure, can be modeled according to the theory of Ref. [4]. Qualitatively, the important feature is this: as the applied pressure increase, a touchdown radius R_{TD} moves from its starting point $R_{membrane}$, at the outer radius of the structure, toward

the center hub. In so moving, however, the stress in the membrane increases, requiring larger, subsequent additions of differential pressure to achieve the same decrease in touchdown radius. As a consequence, the sensor is most sensitive when the applied pressure is near the vacuum reference pressure, between the two capacitor plates.

The central equation used in the description of the sensor behavior is shown in Equation (1). h is the thickness of the membrane. $\epsilon_{tension}$ is the strain induced in the membrane by stretching it over the hub. The coefficients A , B_{linear} , and $B_{tension}$ are related to the remaining structural dimensions, especially the height and radius of the central hub. P is the transmembrane pressure, equal to the difference between the external pressure and the reference pressure.

$$\frac{PR_{TD}^4}{Eh^4} = A \left(\frac{t_{hub}}{h} \right)^3 + B_{linear} \left(\frac{t_{hub}}{h} \right) + B_{tension} \epsilon_{tension} \left(\frac{R_{TD}}{h} \right)^2 \left(\frac{t_{hub}}{h} \right) \quad (1)$$

The model according to Ref. [4] allows calculation of the sensor capacitance as a function of applied pressure. The behavior changes markedly with the height of the hub t_{hub} ; it is also a weaker function of the membrane thickness, the insulator thickness, the membrane radius, and the hub radius. An example is shown in Figure 2. The logarithmic slope of the derivative dC/dP is plotted versus logarithmic pressure, showing a uniform slope which is characteristic of the particular sensor design. In this instance, $t_{hub}=3 \mu m$, $R_{hub}=127 \mu m$, $R_{membrane}=762 \mu m$, $t_{membrane}=1 \mu m$, $t_{ins}=0.2 \mu m$ (nitride).

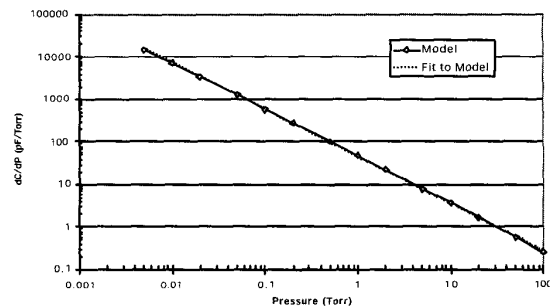


Figure 2: Modeled behavior of the capacitive pressure sensor of Figure 1. The slope of the capacitance vs. pressure curve is related to a simple power law dependence on pressure. The fitting coefficients are functions of the specific sizes of the structural components. Here, the power law slope is -1.1089.

3. Fabrication Process

The major steps in the sensor fabrication process are outlined as follows.

- Starting materials: lightly-doped silicon wafer, polished both sides; Pyrex™ wafer, polished both sides, with via holes.
- Dope one side of the silicon with boron (degenerate doping).
- Pattern the reverse side of the silicon; etch the external pressure surface using KOH (etch stops on p+).
- Deposit, pattern, and etch the reference electrode on the Pyrex™ wafer.
- Metallize the via through-holes. One hole contacts the flexible electrode, while the other contacts the fixed electrode.
- Deposit electrical insulator. This may be deposited on either the fixed or the flexible electrode.
- Bond the silicon and Pyrex™ wafers, using anodic bonding.
- Dice, package, and test.

4. Performance

In order to make practical use of the sensor, electronic signal conditioning and processing is required. Figure 3 shows a schematic of the approach to this problem. A mixed-signal microprocessor is used to facilitate the calibrated conversion of the raw analog output of the sensor and its signal conditioning electronics, into an output signal (either digital or analog) which corresponds to the physical pressure.

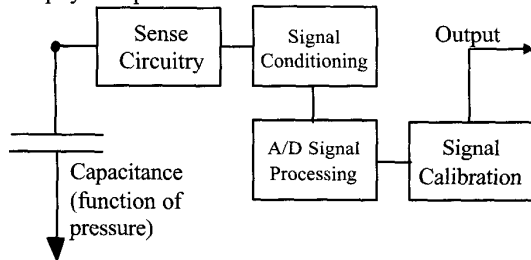


Figure 3: Schematic of the electronics signal processing for the pressure sensor.

Consider a sensor with a vacuum reference pressure. While the sensitivity of the sensor is then greatest near vacuum, the sensor continues to deliver useful, relatively high-resolution data at much higher pressures (see Figure 4). Also, as the silicon membrane is approximately 3 μm thick, and only 1 mm in diameter, its high yield strength allows the

sensor to achieve maximum overrange pressures of at least 200 psig. The upper end of this maximum overrange pressure has not yet been measured.

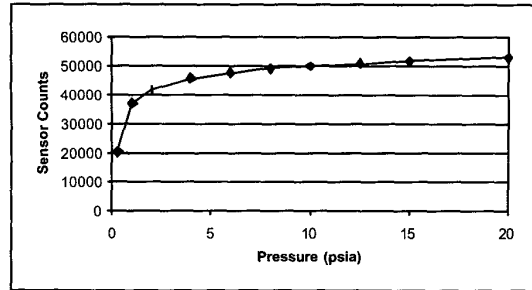


Figure 4: Raw (digital) measurements of the sensor output as a function of input pressure. T=293 K.

The sensor sensitivity is further highlighted in Figure 5. Here, both a capacitive sensor, and an MKS Baratron™ Series 700 sensor, have been mounted on a movable platform. As the platform height varies from 0 to 36" above a reference plane, the barometric pressure decreases. The sensitivity of both sensors can be compared in the figure throughout these height excursions.

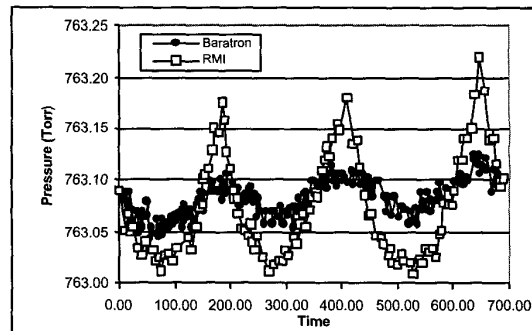


Figure 5: Measurements of ambient pressure reported by two pressure sensors, mounted to a platform cycling through a 36" rise and fall every four minutes.

At the present time, these sensors are being designed into pressure-based MFCs for use in flow control applications where both high dynamic range and high accuracy are required; or, where low inlet pressures are required. We expect to report the results of MFCs fabricated according to these principles in the near future.

5. Discussion

For use as either a unique pressure sensor, or as a component of a mass-flow controller, the sensor must demonstrate a high degree of repeatability. We have

installed these sensors in place of the piezoresistive sensors used in a high-performance MFC [5], and subjected the sensors to variations in pressure, in order to determine the sensor repeatability. Initial results are shown in Figure 6.

“Microfluidic MEMS for semiconductor processing.” *IEEE Transactions on Components, Packaging, and Manufacturing Technology* **B21**, pp. 329-337 (1998).

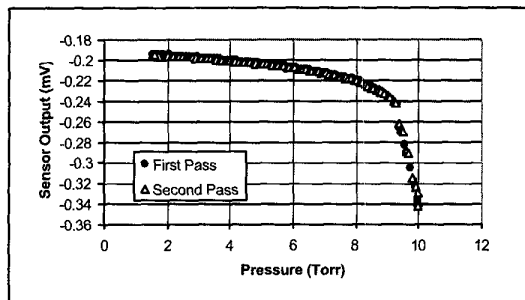


Figure 6: Repeated measurements of the sensor output versus external pressure. The reference cavity pressure is set at 10 T, so that the greatest sensor sensitivity occurs at this pressure. No compensation is made for temperature fluctuations.

6. Conclusions

We have demonstrated a new, silicon capacitive pressure sensor, which has a number of features which make it attractive for use in semiconductor processing application. These features include high sensitivity, operation over a wide pressure range, excellent repeatability, and compatibility with most gases and liquids used in semiconductor processing. The sensor may be used as a standalone device, or in conjunction with the flow sensor in a pressure-based mass flow controller.

Acknowledgements

The authors acknowledge the assistance of L. Schaefer in the electronics design.

References

- [1] J. Bryzek, “Modeling performance of piezoresistive pressure sensors.” In *Proc. 3rd Int. Conf. on Sol.-St. Sens. and Act.*, pp. 168-173 (1985).
- [2] Y. S. Lee and K. D. Wise, “A batch-fabricated silicon capacitive pressure transducer.” *IEEE Trans. Elec. Dev.* **29**, pp. 42-47 (1982).
- [3] A. Zias, *et al.*, US Patent Application
- [4] L. E. Andreeva, *Elastic Elements of Instruments*, Israel Program for Scientific Translations, Jerusalem (1966), pp. 196ff.
- [5] A. K. Henning, “Performance and Reliability of MEMS-Based Gas Distribution Devices.” In *Proc., Gas Delivery and Analysis Symposium* (SEMI, San Jose, CA, 2001); also, A. K. Henning, *et al.*,